ELSEVIER

Journal of Chromatography A, 970 (2002) 141–154

JOURNAL OF CHROMATOGRAPHY A

www.elsevier.com/locate/chroma

Comparison between liquid chromatography–UV detection and liquid chromatography–mass spectrometry for the characterization of impurities and/or degradants present in trimethoprim tablets

Nicolas Barbarin[a], Jack D. Henion[a,*], Yunhui Wu[b]

[a]Analytical Toxicology, Department of Population Medicine and Diagnostic Services, Cornell University, 927 Warren Drive, Ithaca, NY 14850, USA

[b]Department of Pharmaceutical Research and Development, Merck Research Laboratories, P.O. Box 4, West Point, PA 19486, USA

Abstract

The characterization of impurities and/or degradants present in pharmaceutical compounds is an important part of the drug development process. Although LC–UV is commonly employed for impurities and degradant compound determination, LC–MS techniques are proposed in this work to be a viable modern alternative for the characterization of these compounds. LC–UV and LC–MS were compared for the detection of impurities present in different brands of trimethoprim tablets by using an in-line LC–UV–MS system with atmospheric pressure chemical ionization source (APCI) coupled with a reversed-phase gradient HPLC system. It was shown that, although chemical noise was higher when using full-scan LC–MS compared to LC–UV, low level impurities were better detected by mass spectrometry (MS) when modern software algorithms are employed. These included the ‘‘Contour’’ chromatogram algorithm and/or the ‘‘component detection algorithm’’ (CODA). In addition, MS allowed for the simultaneous determination of the molecular masses and some structural information of the impurities and/or degradants. The results also showed a large difference in the purity of trimethoprim among different manufacturers. LC–MS and tandem MS techniques were employed to acquire fragmentation patterns for trimethoprim and its degradants to gain insight into their structures.
© 2002 Elsevier Science B.V. All rights reserved.

Keywords: Mass spectrometry; UV detection; Contour chromatogram algorithm; Component detection algorithm; Trimethoprim

1. Introduction

The detection and identification of impurities and/or degradants present in pharmaceutical formulations plays an important role in the drug development process. The International Conference on Harmonization (ICH), an organization devoted to the coordination of technical requirements for the registration of pharmaceuticals in the United States, Japan and the European Union, has published guidelines on impurities in new drug products and new drug substances [1–3]. These guidelines state that all impurities and/or degradants should be identified when present at a level varying from 1% (for a maximum daily dose of <1 mg) to 0.1% (for a maximum daily dose of >2 g) of the main drug. The

*Corresponding author. Tel.: +1-607-253-3971; fax: +1-607-253-3973.
E-mail address: jdh4@cornell.edu (J.D. Henion).

0021-9673/02/$ – see front matter © 2002 Elsevier Science B.V. All rights reserved.
PII: S0021-9673(02)01035-X

thresholds for an impurity to be reported are even lower and vary from 0.1 to 0.05% (depending upon whether the maximum daily dose is higher or lower than 1 g). Therefore, a single method which allows for the detection, identification and quantitation of very low amounts of impurities in pharmaceutical formulations is needed.

LC–UV, because of its general application, ease of use and low level of chemical and electrical background is still the most commonly used technique for the detection and quantitative determination of impurities present in pharmaceutical compounds. However, its lack of selectivity and the fact that it gives little or no qualitative information on the analytes makes it of little use for identification of unknown impurities or degradants. In addition, impurities are not always detectable by UV [4]. Conversely, full-scan LC–MS allows for the simultaneous detection and molecular mass determination of the analytes while tandem mass spectrometry (MS–MS) provides fragmentation mass spectra which are very useful for structural characterization. However, the possible high level of chemical noise in the total ion chromatogram (TIC) when the mass spectrometer is used in the full-scan mode can be detrimental to the detectability of analytes present at very low levels.

Trimethoprim (TMP), [5-(3,4,5-trimethoxy benzyl)pyrimidine]-2,4 diamine, is a bactericide agent, usually used in association with sulfamethoxazole, for the treatment of urinary tract infections, salmonellosis and chronic bronchitis [5]. It interferes with folate synthesis by blocking the enzyme dihydrofolate reductase which converts dihydrofolic acid to tetrahydrofolic acid. Its structure is presented in Fig. 1. Reports for the study of impurities and/or degradants of TMP are limited. Berghs and coworkers [6–8] described an LC–UV method for the determination of TMP in the presence of five of its degradation products. Those were obtained artificially by exposing the main drug to heat, acidic conditions or direct sunlight. More recently, Dedola et al. [9] studied the photoreactions of TMP in solution and revealed the formation of dimers. Another recent study [10] involved the isolation of two process impurities by preparative liquid chromatography followed by their identification by APCI–MS–MS and NMR. LC–MS has also been used for the determination of TMP itself in bovine serum [11], tissues [12,13] or in water samples [14].

This work presents a comparison between LC–UV and full-scan LC–MS for the characterization of impurities and/or degradants present in three commercial sources of trimethoprim tablets. The ability of both techniques to detect unknown impurities was evaluated and the purity profile of three different brands of TMP tablets was compared. The fragmentation behavior of the main drug was investigated by LC–MS–MS and a fragmentation mechanism was proposed. Using this information, the LC–MS–MS mass spectrum for several detected im-

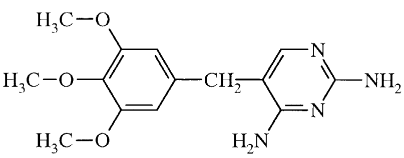

Trimethoprim (MW = 290.1)
$[M+H]^+ = 291.1$

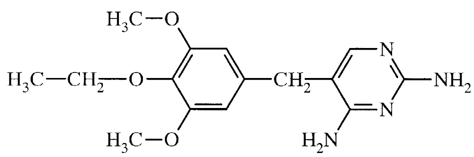

Peak 10 (MW = 304.2)
$[M+H]^+ = 305.2$

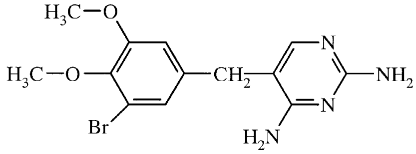

Peak 14 (MW = 338.1)
$[M+H]^+ = 339.1$

Fig. 1. Structure of trimethoprim and its two known process impurities.

purities allowed their structural characterization. Finally, the quantitative determination of impurities obtained by both techniques were also compared.

2. Experimental

2.1. Materials and methods

HPLC-grade methanol was obtained from J.T. Baker (Phillipsburg, PA, USA). HPLC-grade ammonium acetate was from Fisher Scientific (Rochester, NY, USA). Deionized water was generated in-house with a Barnstead Nanopure II filtration system (Boston, MA, USA). Trimethoprim standard (batch 20K1543) was purchased from Sigma (St. Louis, MO, USA).

2.2. Sample preparation

Tablets containing 100 mg of TMP purchased from three different manufacturers were crushed, powdered and dissolved in methanol. The solutions were then sonicated for 10 min and filtered through a 0.45-μm filter. Methanol was added to give stock solutions of 4 mg/ml in 100% methanol. The stock solutions were used to prepare final solutions of 0.6 μg/ml for the determination of the peak area of TMP itself or 0.8 mg/ml for the determination of the impurities.

2.3. In-line LC–UV–MS system

The analyses were performed using an in-line LC–UV–MS system employing an APCI ion source. The chromatographic system consisted of two Shimadzu LC-10AS pumps used in the gradient mode and controlled by the Shimadzu SCL 10A system controller, a Kratos Spectroflow 783 UV detector and a PE Sciex (Toronto, Canada) API 3000 triple tandem quadrupole mass spectrometer. The injection of the samples was performed manually using a Rheodyne (Cotati, CA, USA) 7125 injection valve equipped with a 10-μl loop.

The chromatographic separation was performed on a Keystone (Bellefonte, PA, USA) Betasil 4.6×250 mm C_{18} column, 5 μm particle size. The mobile phase consisted of methanol and a 20-m*M* ammonium acetate aqueous solution with a pH adjusted to 5 with glacial acetic acid. The initial composition of the mobile phase consisted of 75% of the aqueous solution and 25% of methanol. The concentration of methanol was raised to 50% in 20 min and held at that level for 10 min. The analyses were performed at room temperature, at a flow-rate of 1 ml/min. The wavelength of the UV detector was set at 254 nm.

The mass spectrometer was used in the positive ion APCI mode. Data acquisition was performed in the Q1 full-scan mode for the detection of the impurities and in the full scan MS–MS mode for their characterization. The MS parameters were optimized for TMP by infusing a solution of 1 μg/ml at a flow-rate of 10 μl/min in the mobile phase maintained at a flow of 1 ml/min. using a post-column T-connection. The nitrogen nebulizing, curtain and CAD (for MS–MS experiments only) gases were set at 14, 7 and 2 (arbitrary units), respectively, and the auxiliary gas at 4500 ml/min. The APCI discharge needle current was set at 2 μA and the ion source was maintained at 475 °C. For full-scan experiments, the scan range was from m/z 260 to m/z 700 with a step size of 0.5 a.m.u. and a dwell time of 1.5 ms. Preliminary experiments where the full-scan range was set from m/z 200 to m/z 700 showed no evidence for lower mass components, so future experiments were performed with the scan range from m/z 260 to m/z 700 to improve the signal-to-noise ratio. For MS–MS experiments, the collision energy was optimized for each impurity and was either 25 or 30 eV. The mass spectrometer was operated at unit mass resolution in both Q1 and Q3.

During the LC–UV–MS analyses, the main peak for TMP was diverted to waste after the UV detector and prior to entering the mass spectrometer interface in order to avoid saturation of the detector by employing a Rheodyne (Cotati, CA, USA) 7000 switching valve. During the main peak post-column diversion, flow was maintained through the APCI LC–MS interface with a third Shimadzu LC-10AS pump in order to maintain equilibration of the system while the HPLC column effluent was diverted to waste.

UV data were acquired with the Turbochrom 4.1 software and Multiview 1.4 was used for the acquisition of the MS data.

2.4. Quantitative determination of impurities

The impurities were reported as a percentage of the peak areas compared to the peak area of the main drug. Their determination was performed in two steps: a dilute solution of TMP (0.6 μg/ml) was first injected and the extracted ion chromatogram (XIC) peak area was integrated. The peak area obtained was then extrapolated for a concentrated solution (0.8 mg/ml) which was used to determine the peak areas of the impurities. The analyses were performed in three replicates for each formulation.

3. Results and discussion

3.1. Detection of unknown impurities

A comparison between the chromatograms obtained by LC–UV and full-scan LC–MS for the analysis of a representative commercial brand of TMP (brand A) is presented in Fig. 2. In order to avoid saturation of the MS detector, the peak due to the main TMP component was diverted to waste after the UV detector and prior to entering the mass spectrometer. The broad tailing peak detected in the 10–14-min time region of Fig. 2B is the residual of the main component. The UV detector allowed for the detection of 14 peaks: three main impurities (peaks 1, 10 and 14) along with 11 very small but reproducible additional compounds. Although the three main impurities were also well detected by MS, the higher level of chemical noise present in the TIC hindered some very small peaks from being detected. This chemical noise was particularly high following the elution of TMP and can be partially explained by the time required for the evaporation and ionization in the APCI ion source to stabilize after the diversion of the main peak. The use of a third LC pump delivering mobile phase to the mass spectrometer

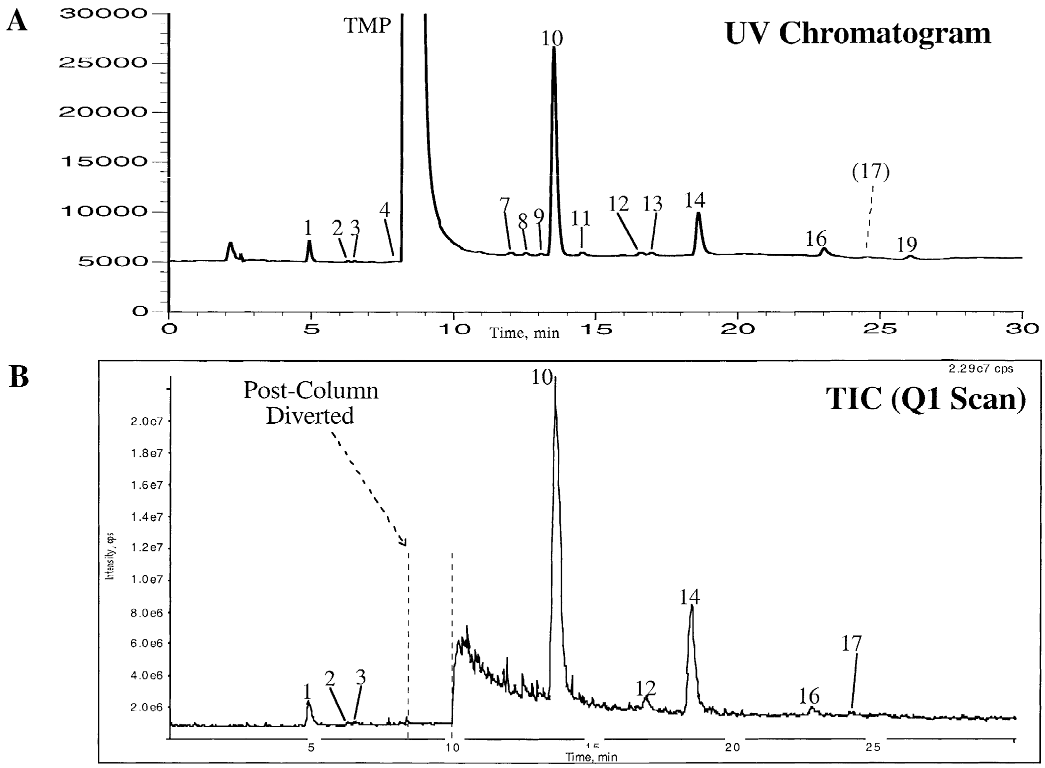

Fig. 2. UV (A) and total ion chromatograms (TIC, B) from the analysis of brand A trimethoprim. The two dashed vertical lines shown in the total ion chromatogram (TIC) in B correspond to the beginning and the end of the post-column diversion.

during the diversion lowered the noise, but not enough to allow the detection of the smallest peaks, especially those eluted just after TMP (peaks 7, 8 and 9 in Fig. 2A).

One way to improved visualization of the small peaks by full-scan MS was to use the Contour chromatogram which is a three dimensional representation of the TIC and a part of the API 3000 Multiview software from PE Sciex (Concord, Ontario, Canada). The Contour chromatogram of TMP (brand A) is presented in Fig. 3. The *x*- and *y*-axes correspond to the time and the m/z values, respectively, and the different colors represent different signal intensities. In this representation, the peaks appear as spots whose coordinates allow for the simultaneous determination of the retention times and the protonated molecule m/z values. In total, 18 impurities were detected among which four (peaks 5, 15, 17 and 18) were not detected by UV. In fact, only one peak (labeled ‘‘7’’ in the UV chromatogram (Fig. 2A)) was not detected in this representation. The intense signal at m/z 291 detected during all the analysis and represented as a broad red line in the Contour chromatogram in Fig. 3 was due to the main tailing peak of TMP. From these results, it was easy to obtain the extracted ion chromatograms (XIC) of any given mass. Fig. 3 shows that peaks 14 and 17 were each observed as two spots of equal intensity. Inspection of the corresponding background subtracted mass spectra (not shown) revealed that each of these species were separated by 2 a.m.u. These species corresponded to the two equally abundant isotopes and revealed the presence of a bromine atom, the relative abundance of ^{79}Br and ^{81}Br being 50:50. Similarly, peak 12 was also represented by two spots. Their different intensity (as shown by the different colors) and inspection of the corresponding background subtracted mass spectrum (not shown) revealed the presence of a chlorine atom, the relative abundance of ^{35}Cl and ^{37}Cl being indeed 75:25.

Another way to improve the detection of the small peaks was to use the component detection algorithm (CODA) described by Windig et al. [15]. Briefly, this algorithm allows for the production of the mass chromatograms with low noise and low background. These mass chromatograms are then combined to form a ‘‘reduced total ion chromatogram’’ trace. The process results in significantly improved chromatograms and allows the detection of small peaks previously lost in the noise. The reduced total ion chromatogram (called ‘‘CODA chromatogram’’ throughout this paper) obtained for the analysis of TMP (brand A) is presented in Fig. 4. The noise was indeed significantly reduced and the small peaks, especially those eluted just after TMP, were easily detected. Even peak 7, the only peak not detected by the Contour chromatogram, was detected in this case and its m/z value of 290.1 was determined. With a m/z value of just 1 a.m.u. less than the main compound, peak 7 was represented in the Contour chromatogram as a spot located just below the intense signal due to TMP and was therefore not visually detected.

The analysis of a second brand of TMP, called brand B, showed a very different purity profile compared to brand A. No impurities were detected either in the UV chromatogram or in the LC–MS TIC. However, the Contour chromatogram allowed for the detection of ten peaks and the CODA chromatogram allowed for the detection of seven peaks (see Fig. 5A,B). Most of the detected impurities were identical to those detected in brand A. Only one new peak (peak 20, m/z=275.1) at a retention time of 15 min was observed.

A third brand of TMP tablets was also analyzed (data not shown). UV allowed for the detection of three impurities while MS allowed for the detection of 12 different peaks by employing the ‘‘Contour’’ and the CODA chromatograms. Again, most of the detected impurities were identical to those detected in the other brands. Only peak 21 (m/z=335.1) had not been detected in the other samples.

The different impurities found in the three brands of TMP, their m/z value and the way they were detected are summarized in Table 1. Among these impurities, compounds 10 and 14 had the same m/z values and the same elution order as the two main process impurities described by Lehr et al. [10], suggesting an equivalent identity. Their structures are presented in Fig. 1. The presence of a bromine atom in compound 14 was confirmed by the presence of two equally abundant isotopes at 339.1 and 341.1. This bromo analog is thought to be formed during the synthesis process and due to the presence of a bromodimethoxy benzaldehyde impurity in the trimethoxy benzaldehyde starting material [16]. Final-

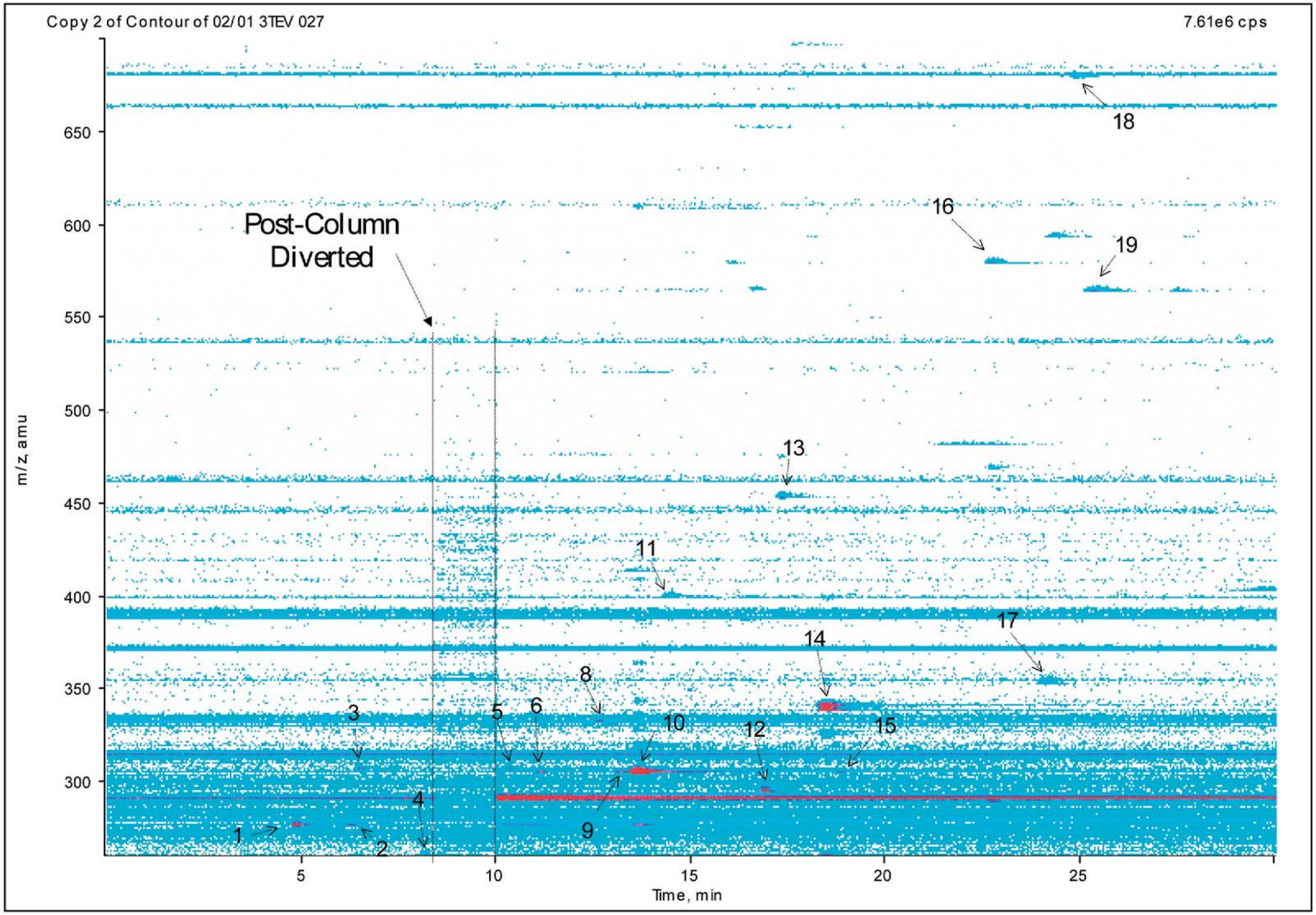

Fig. 3. MS Contour chromatogram from the LC–MS analysis of brand A trimethoprim.

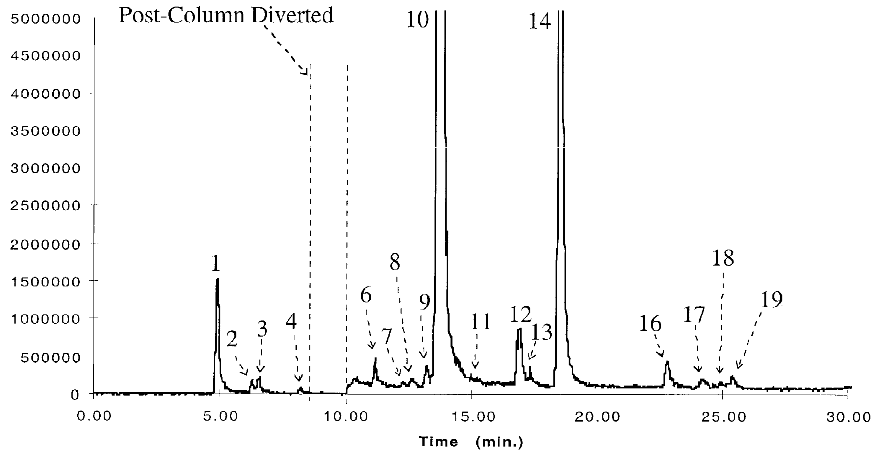

Fig. 4. LC–MS "CODA" chromatogram from the LC–MS analysis of brand A trimethoprim.

ly, peaks 13 and 18 were also detected when mobile phase alone was injected and were not further investigated.

3.2. Identification of unknown impurities

In order to identify the unknown compounds, the fragmentation behavior of TMP and its known impurities were first investigated. The MS/MS spectrum of TMP is presented in Fig. 6 and the fragments obtained for compounds 10 and 14 are listed in the "known compounds" section of Table 2. The results showed that most of the product fragments obtained for TMP and compound 10 were identical, suggesting that the collision-induced dissociation (CID) involved the part of the molecules where the modification occurred. Using this information, tentative fragmentation pathways for TMP were proposed (see Fig. 7). In particular, the presence in both cases of a fragment at m/z 275 suggested the loss of CH_4 (16 a.m.u.) for TMP or CH_3CH_3 (30 a.m.u.) for compound 10. The mechanism of this loss of methane (or ethane) could involve a reaction between two adjacent methoxy groups (path a). Similarly, the presence of a common fragment at m/z 123 suggested a cleavage of the bond located between the central methylene group and the benzene ring and the formation of an ion corresponding to the methylenediaminopyrimidine structure, common to both molecules (path b). The formation of the weak fragment at m/z 81 from the m/z 123 ion was supported by up-front CID [17] of TMP and subsequent fragmentation of the m/z 123 ion (data not shown). It is proposed that this m/z 81 fragment resulted from the loss of NH_2CN and the formation of a four-membered ring shown in Fig. 7 (path b). Conversely, the fragment at m/z 181 was unique to TMP suggesting an ion corresponding to the methylenetrimethyloxyphenyl portion of the molecule (path c). The presence of an ion at m/z 110 in both TMP and compound 10 CID spectra strongly suggested the formation of a fragment corresponding to the diaminopyrimidinium ion (path d). The presence of this ion could possibly involve a charge remote radical cleavage leading to the m/z 110 radical cation and a benzyl radical stabilized by mesomeric effect. CID fragmentations involving radical mechanisms, although rather uncommon, have already been described for quaternary ammonium ions [18] and for eicosanoids [19]. The formation of the m/z 261 ion, also detected for compound 10 and therefore due to the loss of 30 a.m.u. from the para methoxy group, could be explained by the transfer of a hydrogen radical from the methoxy group to the benzene ring resulting in the loss of formaldehyde (path e). It should be noted that the loss of a formaldehyde molecule could occur from either of the three methoxy groups. This conclusion was based on the fact that compound 10 produced two fragments at m/z 275 and 245 which were derived from two successive losses of formaldehyde. Furthermore,

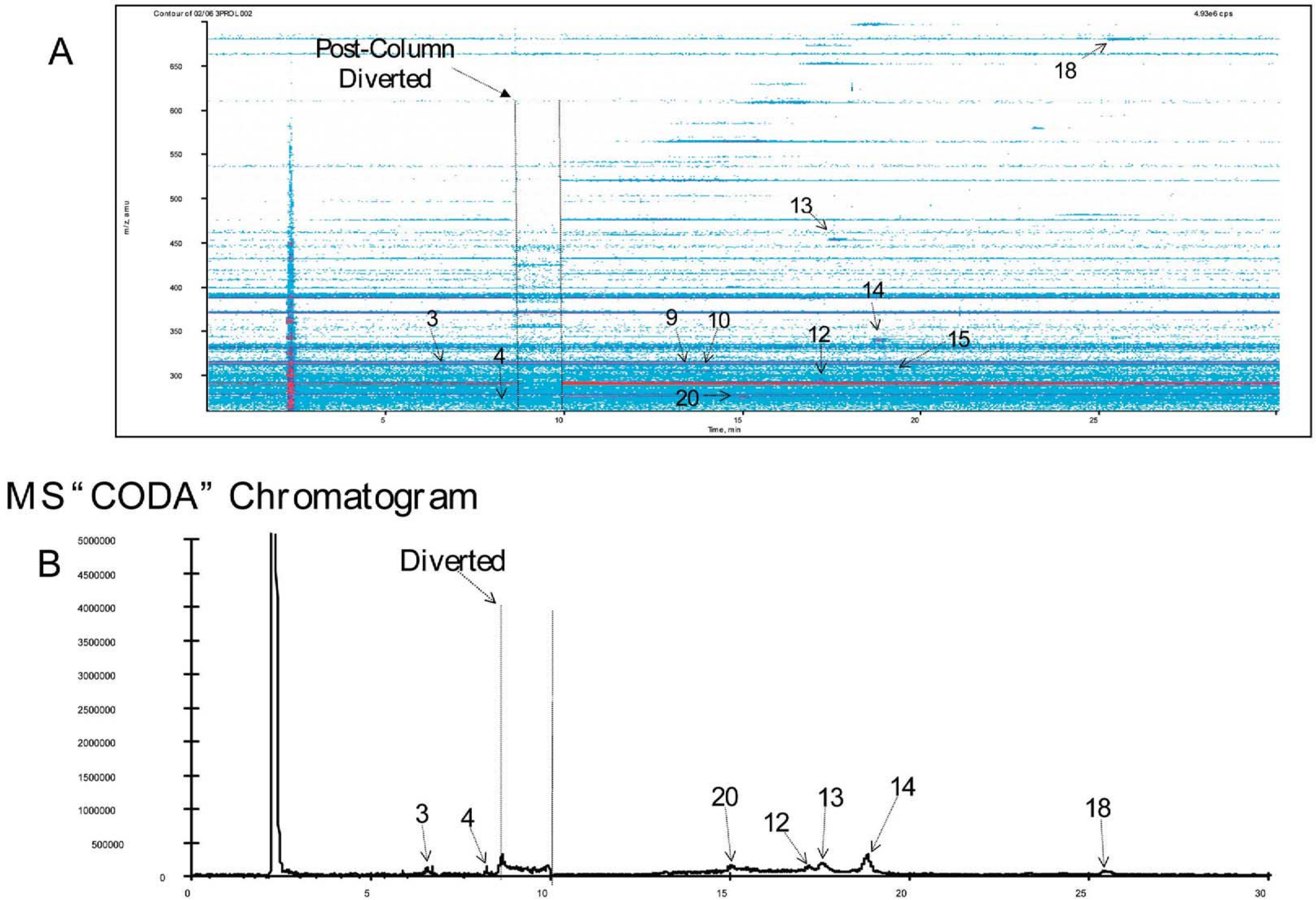

Fig. 5. LC–MS Contour (A) and LC–MS ‘‘CODA’’ (B) chromatograms from the analysis of brand B trimethoprim.

Table 1
Impurities present in two different brands of trimethoprim and the way they were detected: summary

Peak	m/z $(M+H)^+$	Brand A				Brand B			
		UV	MS (Q1 scan)	Contour	CODA	UV	MS (Q1 scan)	Contour	CODA
1	277	+	+	+	+	0	0	0	0
2	277	+	+	+	+	0	0	0	0
3	307	+	+	+	+	−	−	+	+
4	261	+	−	+	+	−	−	+	+
5	307	−	−	+	−	0	0	0	0
6	305	+	−	+	−	0	0	0	0
7	290	+	−	−	+	0	0	0	0
8	333	+	−	+	+	0	0	0	0
9	305	+	+	+	+	−	−	+	−
10	305	+	+	+	+	−	−	+	−
11	400	+	−	+	+	0	0	0	0
12	295	+	+	+	+	−	−	+	+
13*	453	+	−	+	+	−	−	+	+
14	339 341	+	+	+	+	−	−	+	+
15	305	−	−	+	−	−	−	+	−
16	579	+	+	+	+	0	0	0	0
17	353 355	−	+	+	+	0	0	0	0
18*	679	−	−	+	+	−	−	+	+
19	565	+	+	+	+	0	0	0	0
20	275	0	0	0	0	−	−	+	+
21	335	0	0	0	0	0	0	0	0

Peaks 13* and 18* are "system peaks": detected when mobile phase is injected.
+ = impurity present and detected; − = impurity present but not detected; 0 = impurity not present.

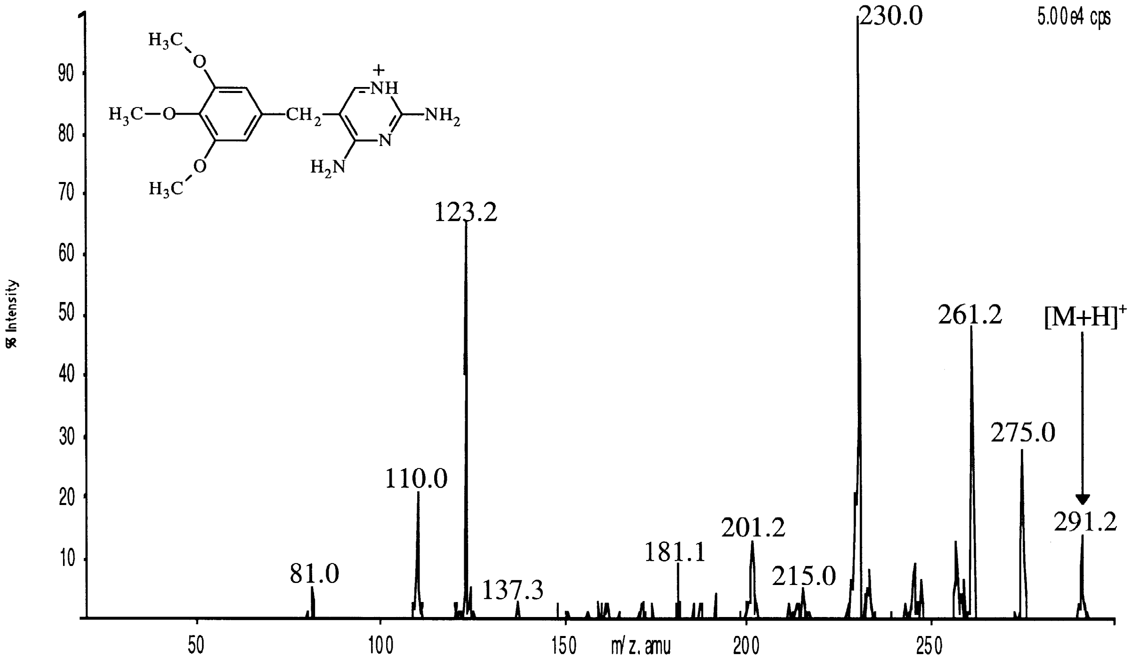

Fig. 6. MS–MS spectrum of trimethoprim.

Table 2
Main fragments obtained by LC–MS–MS of trimethoprim and its impurities and/or degradants

LC peak	m/z $(M+H)^+$	Fragments (m/z)
Known compounds		
TMP	291	275; 261, 230; 215; 201, 181; 159; 137; 123; 110; 81
10	305	275; 261, 257; 245, 230; 201; 186; 123; 110; 81
14	339, 341	232, 325, 295, 297; 244, 229, 231, 216; 123; 110; 81
Unknown compounds		
1	277	261; 233; 216; 187; 123; 110; 81
2	277	261; 233, 123; 110; 81
4	261	245, 123
6	305	289, 271; 244; 215; 137, 123
8	333	316; 291; 275; 261; 230; 123
9	305	275, 261; 230; 123
11	400	384; 370, 339
12	295	279, 251; 234; 216; 123; 110; 81
16	579	469; 289, 273
17	353	323; 244, 123
19	565	456; 418, 180
21	335	319; 289; 275; 261, 230; 167, 123; 100; 81

All fragments are higher than 5% of the base peak.

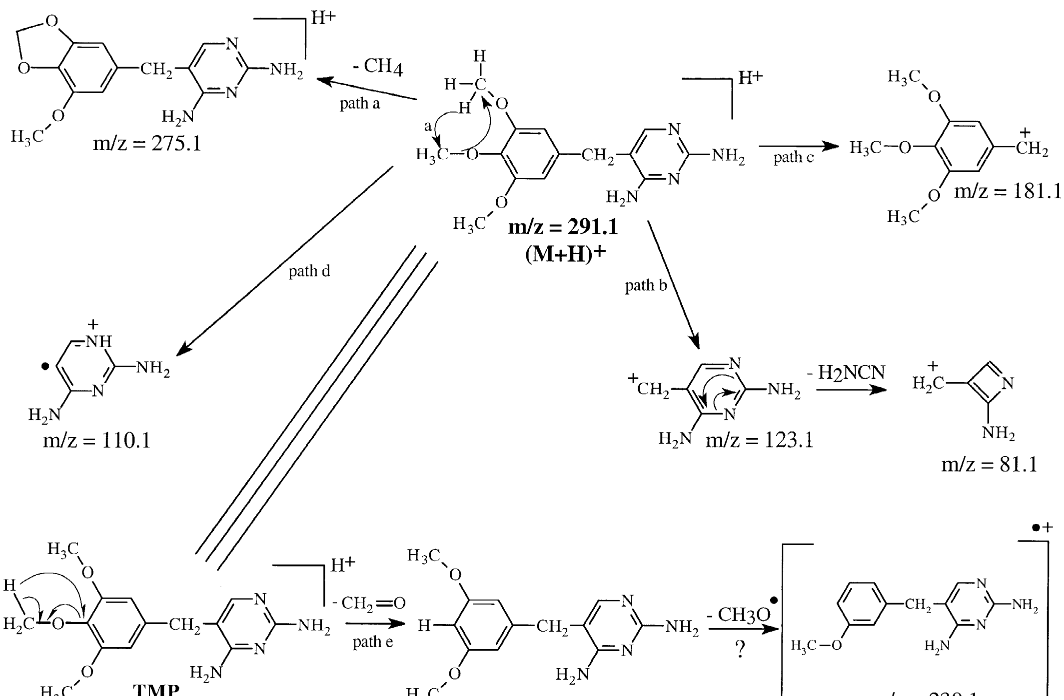

Fig. 7. Proposed MS–MS fragmentation pathways of trimethoprim.

in Fig. 8 was supported by the loss of ethane and the presence of the m/z 123 product ion. In the case of compound 21, the presence of the m/z 275 and 123 product ions, the loss of 16 a.m.u. (methane) and 46 a.m.u. (possibly ethanol) supported the structure proposed in Fig. 8. It must be noted that, in each case, mass spectrometry did not allow the determination of which methoxy group of TMP was substituted. However, because the loss of methane (detected for compound 1, 4, 12, and 21) involved the reaction between two adjacent methoxy groups, the substitution most likely occurred on the third one. Finally, compounds 16 and 19, with m/z values of 579.5 and 565.6, respectively, were proposed to be dimers of TMP. Compound 16 resulted from the association of two TMP molecules and compound 19 from the association of one molecule of TMP and another molecule of TMP where a methoxy group was replaced by a hydroxyl group. The product ions obtained by LC–MS–MS on these two compounds supported the proposed structures and allowed for the proposed fragmentation pathways (see Fig. 9). Compound 16 has already been described as a photodegradation product obtained by exposition of a TMP solution to UV light and its formation involved a radical mechanism [9].

3.3. Quantitative determination

Identification of impurities below the 0.1% level is generally not considered to be necessary unless the potential impurities are expected to be unusually potent or toxic [1–3]. It is therefore very important to determine the quantitative level of the impurities early during the drug development process.

Because reference standards are normally not available for unknown compounds, their quantitative levels are usually expressed as a percentage of the peak area compared to the peak area of the main drug. With this approach, one assumes that the

Compound 16 :

Compound 19 :

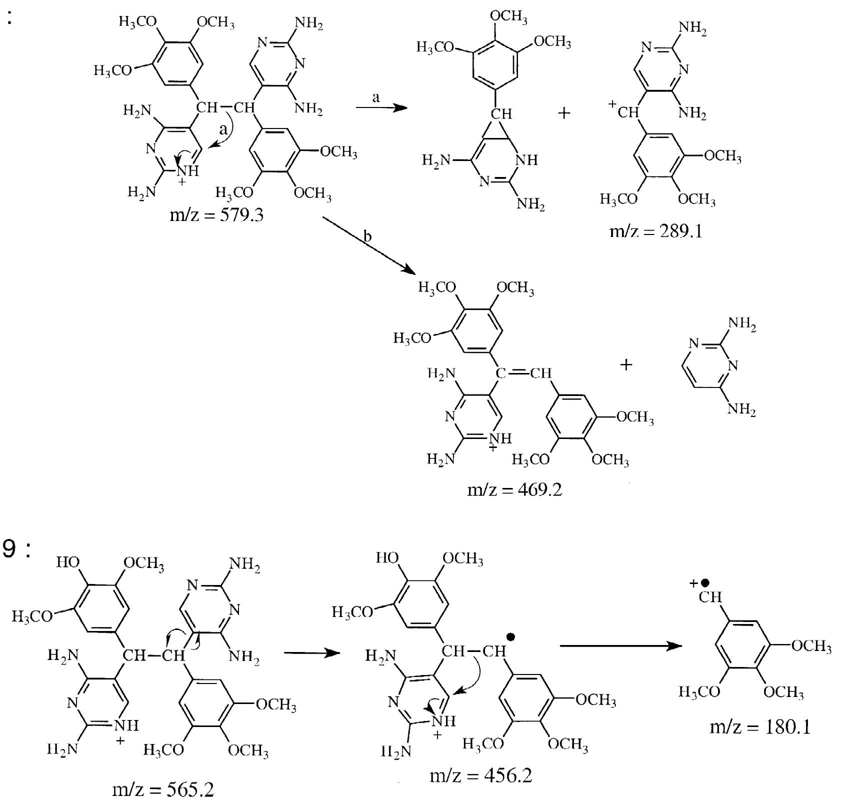

Fig. 9. Proposed fragmentation pathways for dimeric compounds (peaks) 16 and 19.

Table 3
Percentage of impurities present: comparison between UV and MS

LC peak	m/z $(M+H)^+$	% (UV)	RSD for UV (%) (n=3)	% MS	RSD for MS (%) (n=3)
Brand A					
1	277	0.04	1.8	0.03	4.4
2	277	0.0024	3.8	0.0026	0.9
3	307	0.003	3.5	0.0029	5.1
4	261	0.003	21.6	0.002	4.7
8	333	0.0071	7.5	0.0043	6.4
9	305	0.0033	18.0	0.0040	7.7
10	305	0.64	1.1	0.62	3.0
12	295	Co-eluted	Co-eluted	0.014	6.0
14	339,341	0.14	3.3	0.20	5.0
16	579	0.030	3.5	0.009	3.4
17	353,355	Not detected	Not detected	0.006	11.0
19	564	0.014	4.2	0.0036	8.0
Brand C					
1	277	0.005	3.8	0.004	3.0
12	295	Not detected	Not detected	0.001	3.8
14	339,341	Not detected	Not detected	0.003	1.2
20	275	Not detected	Not detected	0.004	3.4
21	335	0.05	0.8	0.04	11.3

impurities and the major component have the same response factors. For UV detection, it means that chromophores should remain intact and for MS detection, that the ionization efficiency remains the same. It was therefore very important to compare the percentages of impurities obtained by both techniques.

Because the detection of low level impurities required the analysis of a concentrated solution of TMP, the UV signal due to the major component was not in the linear working range of the detector. Furthermore, with the peak due to TMP being diverted to waste, no signal was available by MS. Therefore, the level of impurities were determined by analyzing two sample solutions (one concentrated and one dilute) as described in Section 2 and the peak area obtained for TMP at low concentration was extrapolated for the high concentration. The peak areas from LC–MS experiments were obtained from the XICs which allowed to determine area of peaks not detected in the TIC. In the case of compounds containing a bromine or a chlorine atom, one compound corresponded to two masses. Therefore, to allow for a direct comparison with UV, the peak areas of the two isotopes were determined separately and added.

The results obtained for the major impurities are presented in Table 3 and show that the percentages obtained by both detection techniques were close to each other for most of the impurities. The difference in structures between TMP and its impurities should not greatly affect the UV response factors since the chromophores remain the same. Furthermore, because the ionization in the APCI ions source most likely occurred on the pyrimidine ring, a substitution of a methoxy group by another group should not greatly affect the ionization efficiency either. It is therefore not surprising that the percentage composition determined by both techniques were similar.

However, for some other compounds, the results were different. For instance, the levels of the two dimers (compounds 16 and 19) determined by MS were, respectively, three and four times lower than those obtained by UV. Conversely, the compounds containing a halogen atom (bromine or chlorine) seemed to be better detected by MS resulting in determination of higher levels. The fact that dimers have twice the number of chromophores resulted in higher UV response factors and could partially explain the difference in levels determined by the two detectors. However, this difference in the UV response factors could not justify a difference of 3 or

4 in the values and suggested that the MS response factors were lower than the one of TMP. Possible reasons could involve fragmentation of the dimers occurring in the APCI source maintained at 475 °C or the fact that MS parameters were optimized for TMP and not for these much larger molecules. The higher percentages obtained by MS for the halogenated molecules remain unclear. The substitution of a methoxy group by a electron withdrawing group via inductive effect (halogen atom) could influence the UV response factors leading to inaccuracies of the amounts actually present.

The use of the XICs resulted in lower detection limits and allowed for the quantitative determination of compounds present in very low amounts and not detected by UV (brand C, compounds 12, 14, 20, for example). Most of the impurities detected were well below the level of 0.1% where identification is required. In fact, only compounds 10 and 14 in brand A were present above this level.

4. Conclusions

Although chemical noise was higher when using full-scan LC–MS compared to LC–UV, very low level impurities were better detected by MS due to the use of the Contour chromatogram and/or the component detection algorithm (CODA). In addition, LC–MS allowed for the simultaneous determination of the impurity and/or degradant molecular masses plus some structural characterization.

The determination of the percentage of impurities obtained by LC–UV and LC–MS gave similar values for most of the compounds. However, the level of the dimers appeared to be higher with UV. Conversely, the level of the compounds containing halogen atoms (Br or Cl) were higher when determined by MS. This could lead to an over or under estimation of the quantities of these impurities actually present.

Large differences in the total amount of impurities were detected from one manufacturer to another. The use of tandem mass spectrometry allowed for the proposal of fragmentation pathways for TMP and subsequent structures for the unknown impurities. Finally. mass spectrometry is well-suited for both detection and characterization of impurities and/or degradants present in pharmaceutical compounds at levels well below those where detection and identification are required.

Acknowledgements

The authors gratefully thank Dr W. Windig and Eastman-Kodak for data analysis with the component detection algorithm (CODA) and PE Sciex for the generous loan of the API 3000. NB thanks Dr Timothy Wachs for many helpful discussions, Merck Research Laboratories and the Catholic University of Louvain for financial support.

References

[1] ICH, International Conference on Harmonization Guideline. Q3A: impurities in new drug substances, 1995.
[2] ICH, International Conference on Harmonization Guideline. Q3B: impurities in new drug products, 1996.
[3] ICH, International Conference on Harmonization Guideline. Draft Consensus Guideline: impurities in new drug substances, 1999.
[4] S.D. McCrossen, D.K. Bryant, B.R. Cook, J. Pharm. Biomed. Anal. 17 (1998) 455.
[5] Martindale's, The Extra Pharmacopia, 27th ed, Pharmaceutical Press, London, 1979, 361.
[6] J.J. Bergh, J.C. Breytenbach, J. Chromatogr. 387 (1987) 528.
[7] J.J. Bergh, J.C. Breytenbach, P.L. Wessels, J. Pharm. Sci. 78 (4) (1989) 348.
[8] J.J. Bergh, J.C. Breytenbach, J.L. Du Preez, J. Chromatogr. 513 (1990) 392.
[9] G. Dedola, E. Fasani, A. Albini, J. Photochem. Photobiol. A 123 (1999) 47.
[10] G.J. Lehr, T.L. Barry, G. Petzinger, G.M. Hanna, S.W. Zito, J. Pharm. Biomed. Anal. 19 (1999) 373.
[11] P. Nachilobe, J.O. Boison, R.M. Cassidy, A.C.E. Fesser, J. Chromatogr. 616 (1993) 243.
[12] A. Cannavan, S.A. Hewitt, S.D. Floyd, D.G. Kennedy, Analyst 122 (1997) 1379.
[13] S. De Baere, K. Baert, S. Croubels, J. De Busser, K. De Wasch, P. De Backer, Analyst 125 (2000) 409.
[14] R. Hirch, T.A. Ternes, K. Haberer, A. Mehlich, F. Ballwanz, K.-L. Kratz, J. Chromatogr. A 815 (1998) 213.
[15] W. Windig, J.M. Phalp, A.W. Payne, Anal. Chem. 68 (1996) 3602.
[16] F. De Martilis, E. Ciranni-Signoretti, G. De Marchi, M. Lunardelli, G. Sekules, A. Zanotti-Gerosa, Boll. Chim. Farm. 122 (1983) 462.
[17] K.L. Duffin, T. Wachs, J.D. Henion, Anal. Chem. 64 (1992) 61.
[18] C. Seto, J.S. Grosset, D.S. Waddell, J.M. Curtis, R.K. Boyd, J. Am. Soc. Mass Spectrom. 12 (2001) 571.
[19] J.M. Hevko, C. Murphy, J. Am. Soc. Mass Spectrom. 12 (2001) 763.